Antenna-Coupled Transition-edge Hot-electron Micro-Bolometers

S. Ali[a], P. T.Timbie[a], S.Malu[a], D.McCammon[a],K.L.Nelms[a],
R.Pathak[a], D.van der Weide[a]
C.A.Allen[b], J.Abrahams[b], J.Chervenak[b], W.T. Hseih[b],T.M.Miller[b],
S.H.Moseley[b],T.R.Stevenson[b] and E.Wollack[b]

[a]University of Wisconsin-Madison, Madison, WI 53706,USA;
[b]NASA Goddard Space Flight Center, Greenbelt, MD 20771,USA

ABSTRACT

We are developing a new type of detector for observational cosmology and astrophysical research. Incoming radiation from the sky is coupled to a superconducting microstrip transmission line that terminates in a thin film absorber. At sub-Kelvin temperature, the thermal isolation between the electrons and the lattice makes it possible for the electrons in the small absorber (100's of μm^3) and superconducting bilayer (Transition Edge Sensor) to heat up by the radiation absorbed by the electrons of the normal absorbing layer. We call this detector a Transition-edge Hot-electron Micro-bolometer (THM). THMs can be fabricated by photo lithography, so it is relatively easy to make matched detectors for a large focal plane array telescope. We report on the thermal properties of Mo/Au THMs with Bi/Au absorbers.

Keywords: Microbolometer,Hot-electron;Superconducting sensors

1. INTRODUCTION

The anisotropy and the polarization of the cosmic microwave background (CMB) contain a wealth of information about the early universe. Recently the WMAP[1] satellite has mapped the full sky CMB anisotropy with unprecedented precision. The polarization of the CMB has also been detected by the DASI[2] and WMAP.[3] The era of measuring the CMB polarization is only starting. Further improvements in the measurements of the CMB polarization will improve our understanding of the cosmological parameters and probe the era of inflation. The CMB polarization signal is at a level 10% of the CMB anisotropy signal. Both instrumental and observational techniques have to be developed to precisely measure such a small signal.

The detectors used for CMB experiments are already background limited; the way to improve on sensitivity is to make large format detectors arrays. Promising candidates for this application include bolometers that use a Transition edge Sensor (TES) as a thermistor. A thin superconducting film is maintained at the middle of its superconducting - normal transition by negative electro-thermal feedback.[4,5] RF power heats the bolometer and changes the TES resistance and thus the feedback current. Highly sensitive SQUID amplifiers are used to read out these bolometers. Here we describe a type of TES bolometer called a Transition-edge Hot-electron Microbolometer (THM).

2. TRANSITION-EDGE HOT-ELECTRON MICROBOLOMETER

TES devices have proved to be a lot faster than the conventional Neutron-Transmutation-Doped (NTD) or doped Si bolometers. TES bolometers are a close match for the NTD bolometers in sensitivity. In addition TES bolometers can be fabricated lithographically and multiplexed making them highly suitable for large array formats.

We are building a type of TES bolometer we call Transition-edge Hot-Electron Microbolometer (THM). A small TES is in thermal contact with a normal metal absorber. The electrons in the normal metal absorber are heated by incident radiation. The weak electron-phonon thermal coupling in metals at low temperature allows the the temperature of the electrons in the adjacent TES to rise for a small change in absorbed power. The thermally active area for the antenna coupled bolometer can be much smaller than the wavelength of

Millimeter and Submillimeter Detectors for Astronomy II, edited by
Jonas Zmuidzinas, Wayne S. Holland, Stafford Withington, Proceedings of
SPIE Vol. 5498 (SPIE, Bellingham, WA, 2004) · 0277-786X/04/$15 · doi: 10.1117/12.552836

the radiation of interest. In our design the absorber is separate from the TES which allows us the flexibility of optimizing the two components independently. The absorber resistance can be varied such that it is well matched to the antenna impedance (10′s of Ω) while the TES impedance can be matched to the low SQUID amplifier readout ($< 1\ \Omega$). Hot-electron effects in ultrathin films have been demonstrated by Gershenson et al.[6] in devices called Hot-electron Direct Detectors (HEDD). In HEDD devices the TES also acts as the absorber.

Figure 1 shows a schematic of a THM coupled to a superconducting microstrip line. The bottom figure is a thermal circuit for the THM. A normal metal (heater/absorber) terminates the microstrip line. For efficient power transfer the impedance of the heater/absorber must be matched to that of the transmission line. Andreev reflections[7] at the superconducting leads keep the hot electrons in the TES and the heater/absorber from escaping down the superconducting leads. The internal heat conductivity of the TES is given by the Weidemann-Franz law[8] $G_{\rm WF} = L_0 T/R$, where $G_{\rm WF}$ is the thermal conductance from one end of the film to other, T is the temperature of the electrons in the film, R is the electrical resistance from one end of the film to the other, and $L_0 = (1/3)(\pi k_{\rm B}/e)^2 = 2.44 \times 10^{-8}\ {\rm W\Omega/K^2}$ is the Lorenz number. For the heater/absorber to be isothermal, we require $G_{\rm WF} >> G_{\rm ep}$. Here, $G_{\rm ep} = dP_{\rm ep}/dT = 5\Sigma V T^4$, where, $P_{\rm ep} = \Sigma V(T^5 - {T_{\rm p}}^5)$, and Σ is a constant that depends on the material, V is the volume of the metal, and T and $T_{\rm p}$ are the temperatures of the electrons and the phonons respectively.[9]

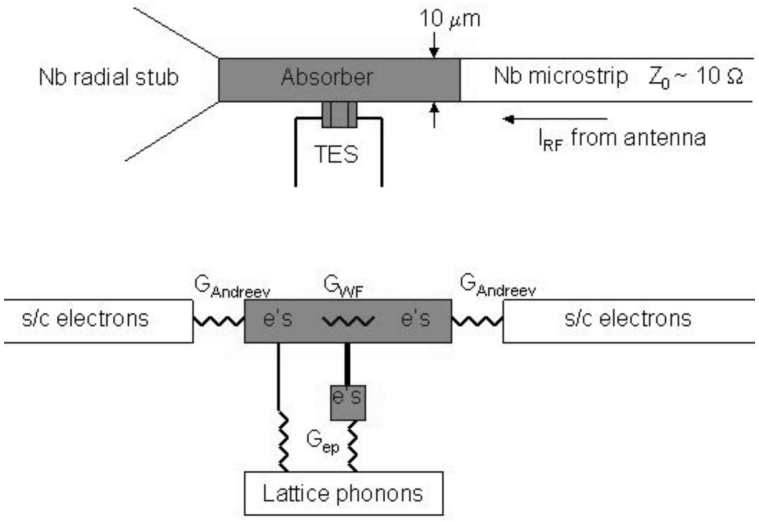

Figure 1. Top figure shows a resistive normal metal film acting as a termination of a microstrip transmission line with an impedance of $\sim 10\ \Omega$. The film overlaps an adjacent TES sensor and forms electrical and thermal contact with it. Bottom figure is a schematic of the thermal circuit for the THM. In order to treat the electrons as isothermal, we require the internal thermal conductivity of the absorber (and TES) to be much greater than the electron-phonon conductivity (i.e. $G_{\rm WF} >> G_{\rm ep}$.) In addition, $G_{\rm ep}$ is chosen so that the thermal fluctuations in electron-phonon thermal link are small compared to the photon noise from the observed source.

3. PLANAR ANTENNA

One of our goals is to couple radiation from free space directly into the normal electrons in the superconducting film of a TES. A wide range of planar antennas are suitable for coupling to millimeter and submillimeter wave detectors. Radiation collected by planar slot antennas can be transmitted through superconducting striplines to the bolometric detectors without appreciable loss in signal; which make them suitable for detecting small signal such as the CMB polarization radiation. Planar double slot antennas are particularly useful because they produce nearly Gaussian beams. A pair of dual slot antennas oriented at 90 to each other will couple to two orthogonal polarizations which makes them a perfect choice for polarization measurements. Several research groups[10,11] are also developing designs to couple TES devices to polarization-sensitive planar antennas. We

plan to fabricate the slot antennas on a Si wafer by patterning a Nb/SiO/Nb structure, where the groundplane and the microstrip transmission lines are separated by a layer of insulator (SiO). The beam width of the planar antenna can be adjusted by placing the antenna on a thick hyperhemispherical silicon lens.[12] The lens maintains the gaussicity and the directivity of the beam pattern and suppresses substrate modes. We propose to couple THMs to a dual-polarization antenna formed from a pair of crossed dual-slot antennas. Microstrip lines couple from the antennas to the microbolometers. Each antenna resonates at a specified frequency, but additional filtering can be achieved with standard microstrip bandpass filters. The bias/readout lines from each THM include microstrip low-pass filters to prevent the RF signal from escaping from the detector. The Stokes Q parameter is proportional to the difference between the signals measured by the two detectors and the intensity, I, is proportional to the sum. When rotated by 45° this antenna pair measures the Stokes U parameter.

4. FABRICATION

Here we outline the procedures used in the fabrication of the THM devices we have studied.[13] All devices are from the same unoxidized four inch Si wafer. The detector element consists of a molybdenum-gold bilayer deposited in a vacuum system with a background pressure of 2×10^{-7} torr. The wafer surface is cleaned in situ with a reverse bias argon plasma. Then, a 40 nm layer of Mo followed by a 150 nm layer of Au are sputtered without breaking vacuum. The sample is removed from the chamber and annealed at 150°C to circumvent aging effects. The Au layer is patterned into the shape of the THM detector element are dry-etched via ion milling down to the Mo layer. The Mo is then patterned into wiring [Fig. 2] for the THM and leads for the heater/absorber element and reactive ion etched down to the Si substrate. The edges of the THM are defined by a second ion mill and RIE to prevent a superconducting short along the edges of the detector. Finally, a Bi/Au layer (500 nm/200 nm) is thermally evaporated through a liftoff photoresist mask to create the resistor for the heater/absorber element. Au was applied on top of the Bi layer to stabilize the heater/absorber layer. Subsequent resistance measurements have shown that Bi/Au is not as stable as the Bi/Cu system *.

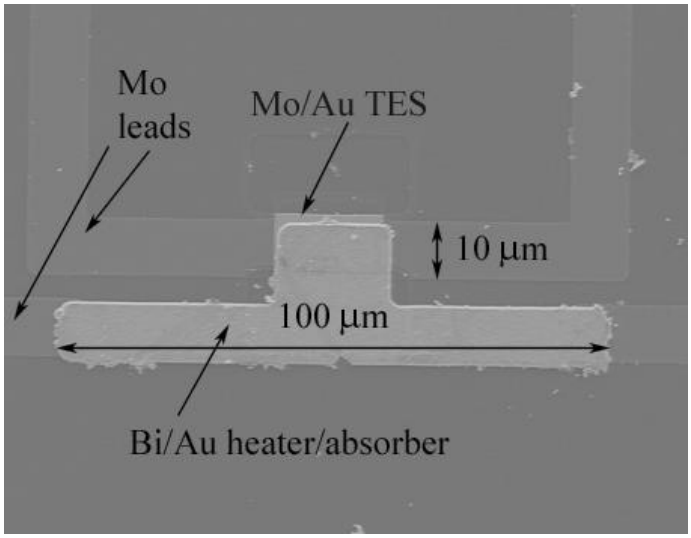

Figure 2. SEM image of a 10 μm by 20 μm THM device with Bi/Au absorber. The TES is made from a proximatized bilayer of 40nm of Mo and 150nm of Au. The bottom Mo layer has been patterned to make the superconducting leads for the TES device and the overlapping Bi/Au absorber.

5. EXPERIMENTAL SETUP

We have conducted tests of THM devices in the dark (i.e. without any incoming radiation on the detectors). By means of the typical measurements we make on conventional TES devices, we test our thermal model of the

*Naoko Iyomoto Private communication.

hot-electron devices and measure noise. Measurements include resistance-versus-temperature, current-versus-voltage, noise spectra, and TES resistance as a function DC current in the absorber. By recording the DC bias power required to heat the electron system to the TES transition temperature as a function of the substrate temperature, we measure the electron-phonon thermal conductivity. We have tested the thermal properties of four THM test devices. All four test THMs have the same geometry. Each of the devices is 10 μm by 20 μm with 10 μm wide Mo leads. Two of the test devices (THM01 and THM03) have no absorbers and two of them (THM02 and THM04) have Bi/Au absorbers. The Bi absorbers are 10 μm $\times$ 100 μm and also have 10 μm wide Mo leads. The measurements are taken in a cryostat equipped with an adiabatic demagnetization refrigerator (ADR). The thermal properties were measured with the THM biased in both constant current and constant voltage modes.

5.1. 4 wire measurement

To date we have measured the R vs T characteristics of four THM devices by constant current bias mode. The THM devices are epoxied to a small Cu sample holder. The THM devices are wire bonded to copper pads on the sample holder. The whole assembly is enclosed in a Nb can for reducing magnetic interferences from the ADR and the environment. The Nb can housing the THMs is attached to the coldstage. The R versus T curves were taken by biasing the TES devices by a AC bias current at 17Hz with bias currents ranging from 0.3μA to 3.0μA. The voltage drops across the TES were measured with a lockin amplifier. We also repeated the 4 wire measurement by DC biasing the TES devices.

To measure the thermal conductivity a DC battery box was used to send a current through the Bi absorber that overlaps the AC-biased TES. The TES device was AC-biased with a small current and the power through the Bi absorber was varied. The THM went through its transition as the bath temperature was varied. Increase in power to the heater/absorber shifted the T_c to lower temperature.

5.2. Voltage bias measurement

In the second cooldown, THM02 was wired up to a Quantum Design DC SQUID through a voltage bias circuit. A 26 mΩ resistor was used as a shunt resistor. The THM and the shunt resistor was biased by a DC battery box power supply. The THM was housed inside another Nb can and heat sunk to the cold-stage. A pair of twisted superconducting Nb-Ti wires connected the THM circuit to the input coil of a Quantum Design DC SQUID . The twisted Nb-Ti wires were shielded by a stainless steel tube coated with with Pb. The SQUID assembly with it's magnetic shielding is attached to the $4K$ stage.

5.3. Time constant Measurements

To measure the time constant of the THMs pulses were passed through the Bi/Au heater/absorber of THM04. Using a 4-wire connection to the TES, the TES was biased with a DC current, and the TES response was measured with an oscilloscope. The Bi pulse polarity was reversed to ensure that the TES response was thermal rather than electrical in nature.

6. RESULTS

The transition temperatures of the THM devices were found to be very similar to each other. Table 1 lists the normal resistances and the T_cs for each of the four devices measured. The thermal conductivity of the electron-phonon system was measured with several different methods. In the first method a DC current is passed through the absorber. THM02 and THm04 were AC biased by 0.6 μA of current. The ADR cold stage temperature was varied through the transition temperature of the TES devices. The R vs T curves shifted to lower temperatures as the current through the absorber was increased as expected (see figure 3). Tables 2 and 3 list the power through the Bi absorbers and the computed G values. In the second method the cold stage temperature was maintained in the middle of the TES transition and a small amount of DC power was allowed to heat up the AC-biased TES. A typical G value calculated from this measurement ($1.6\times10^{-8}W/K$) is similar to the value calculated from the previous method.

The time constant of THM02 measured from the pulse Bi current is less than 30 μs. This is an upper-limit for the time constant expected from electron-phonon decoupling in these devices.[14] We were limited by the stray capacitance in our read out system to make a more precise measurement at this time.

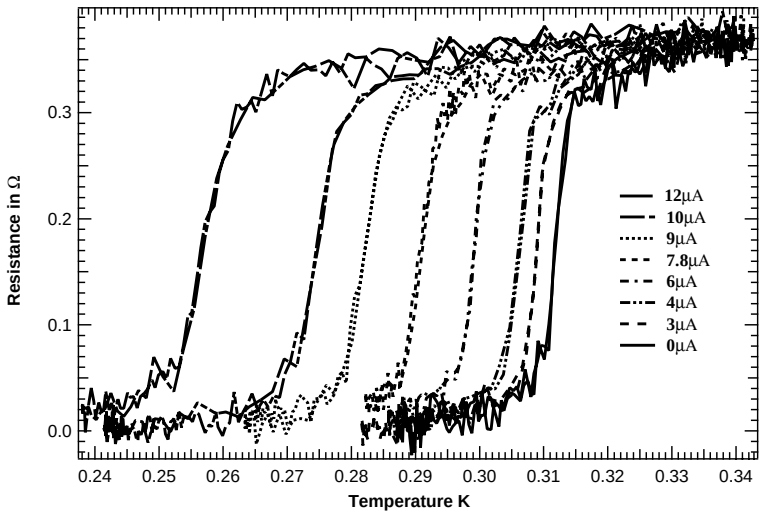

Figure 3. The R vs T curves for TES02 with different dc currents through the Bi heater/absorber. The test device was biased with a constant AC bias current (0.6μA) while the absorber was heated by a dc current. The absorber has a resistance of 7 ohms. A value for G can be calculated from this data which is consistent with the electron-phonon decoupling model.

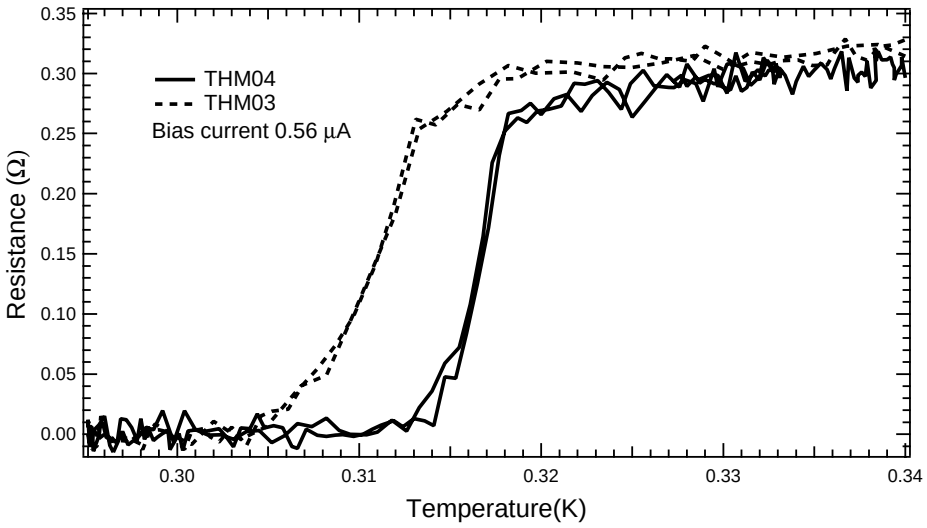

Figure 4. The R vs. T curve for two of the test pieces. Both of the TES devices have the same dimensions. The devices were biased with an constant AC bias current (0.56μA) and the bath temperature was varied through the Transition temperature of the devices.

7. DISCUSSION

The measured values of G are consistent with published values of $G_{\rm ep}$ for Bi and Au, the materials that dominate the volume of the fabricated devices. See Table 4. Summing the values of $G_{\rm ep}$ for Au and Bi at $T_{\rm c} = 0.310$ K gives $G_{\rm ep} = 2.9 - 4.5 \times 10^{-8}$ W/K, in good agreement with our measured value of $\sim 2 \times 10^{-8}$ W/K. Measurements at lower temperatures are required to determine whether $G \sim T^4$ as expected for the electron-phonon interaction in metals in the thick film limit (see figure 6). These measurements would require fabrication of devices with lower values of $T_{\rm c}$ and are planned for the future.

Table 1. The Transition temperatures and the normal resistances of the 4 TES devices are listed. THM01 and THM03 are without any absorber while THM02 and THM04 have Bi absorbers. THM02 was measured with both constant current and constant voltage. Note that the T_c measured in the voltage biased circuit is lower than that measured in the current biased circuit.

	Resistance Ω	T_c mK
THM01	0.331	314
THM02	0.350	311
THM03	0.320	310
THM04	0.298	316
THM02[a]	0.39	295

[a]Measured in constant voltage bias mode.

Table 2. A DC current was maintained through the Bi absorber of THM02 while the TES was AC-biased. Thermal conductivity was measured by measuring the shift in T_c.

Bi Resistance Ω	Current μA	G W/K
7.3	7.8	2.14×10^{-8}
7.3	6.0	2.15×10^{-8}
7.3	4.0	2.049×10^{-8}
7.3	3.0	2.43×10^{-8}

Table 3. Similar table for THM04.

Bi Resistance Ω	Current μA	G W/K
4.2	9.0	1.75×10^{-8}
4.2	7.0	1.79×10^{-8}
4.2	5.0	1.85×10^{-8}
4.2	3.0	1.64×10^{-8}

The value of $G_{\rm WF}$ is also computed for the THM based on the measured values of the resistance of the films. For the absorber and the TES to be in thermal equilibrium with themselves and each other, $G_{\rm WF} > G_{\rm ep}$. Table 4 indicates that this is approximately true.

Expected values of the thermal time constant, $\tau_{\rm ep} = C_{\rm e}/G_{\rm ep}$ are given in Table 5. The computed value of $\tau \sim 0.1$ μs is consistent with our measured upper limit of $\tau < 30$ μs. A time constant of ~ 30 μs is expected at 0.1 K (Figure 7).

Future devices will be fabricated to operate at lower temperatures in order to reduce $G_{\rm ep}$ and hence the phonon noise contribution to the sensitivity of the THM. Lower values of $T_{\rm c}$ can be obtained by increasing the thickness of the Au layer relative to the Mo layer in the TES. Assuming the thermal conductance is dominated

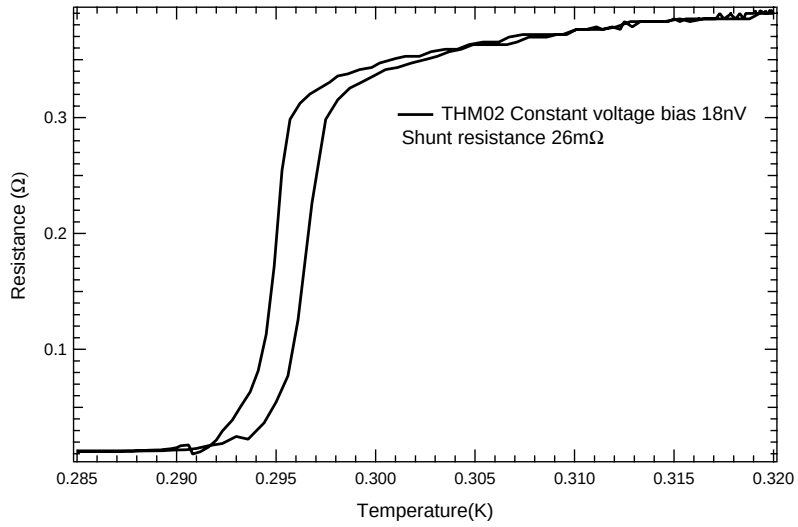

Figure 5. The R vs. T curves for THM02 measured with a DC SQUID in constant voltage bias mode. The transition curves show hysteresis between the warming and the cooling legs; and the T_c is lower than that measured with the 4 wire measurement. A value for α ($\frac{T}{R} \times \frac{dR}{dT}$) can be calculated from the slopes of these curves. The average value of α is 195.

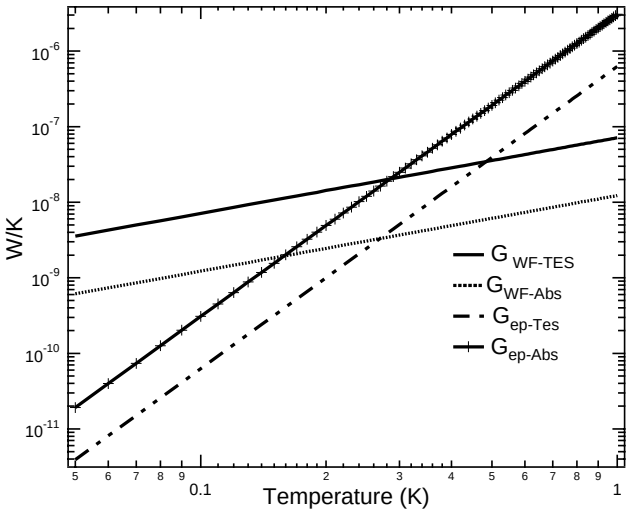

Figure 6. Predicted thermal conductances for the THM devices. $G_{\rm ep\ TES}$ and $G_{\rm ep\ Abs}$ are the electron-phonon thermal conductance for the TES itself and the heater/absorber respectively. Both are assumed to have a T^4 temperature dependence. The measured value of G at 0.310 mK is close to the predicted value. $G_{\rm WF\ TES}$ and $G_{\rm WF\ Abs}$ are the Wiedemann-Franz thermal conductivities along the length of the TES and the heater/absorber respectively.

by $G_{\rm ep}$ and scales as T^4, a value of $G_{\rm ep} \sim 10^{-10}$ can be achieved at $T \sim 0.1$ K (Figure 6). As mentioned above, these values of G and T are appropriate for background-limited observations of the 2.7 K CMB.

8. CONCLUSION

THM devices have been fabricated with Bi/Au absorbers in contact with TES made of Mo/Au bilayers. The measured thermal conductivity and time constant are in good agreement with those expected from the electron-phonon interaction in the metal films. Devices of this type with either smaller volume or lower values of T_c will

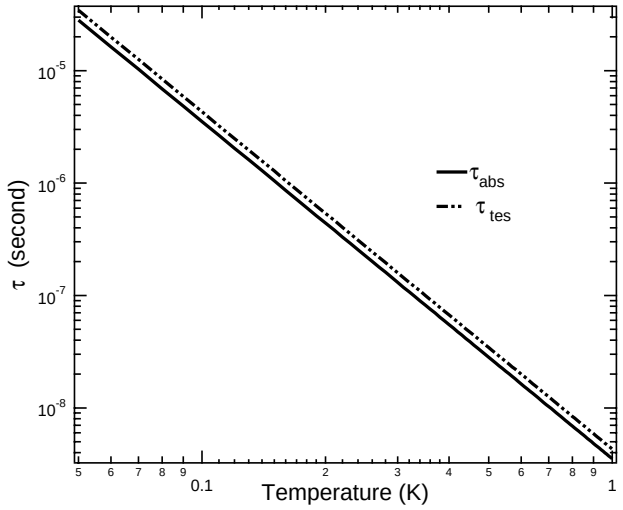

Figure 7. Predicted thermal time constant of the THM. $\tau_{\rm ep\ TES}$ and $\tau_{\rm ep\ Abs}$ are the time constants of the TES and the heater/absorber respectively. By chance, they are nearly identical. The upper limit on the time constant of the THM at 0.310 K is consistent with the predicted value.

Table 4. Expected values of the electron-phonon thermal conductance, $G_{\rm ep}$, and the Wiedemann-Franz thermal conductance along the length of the films, $G_{\rm WF}$. Calculations are based on data from the literature as noted. All devices have nominally the same dimensions, $L \times w \times t = V$. Note that the heater/absorber is a bilayer of Bi (500 nm) and Au (150 ± 50 nm); both are included in the calculation here. The TES is a bilayer of Mo and Au; the thickness of the Mo is small (40 nm) compared to the Au (150 nm) so we have neglected it here and pretend that the entire TES is a Au layer of 190 nm thickness. Values for Σ for Au are from Pierre et al.[15] For Bi in the "pure" (thick film) limit Dorozhkin et al.[16] measure $\tau_{\rm ep} = 3.4 \times 10^{-10} T^{-3}$ for $0.3 < T < 2$ K, so $G_{\rm ep} = C_{\rm e}/\tau = 1.2 \times 10^9 T^4 V$, giving Σ as shown below. The values of G are calculated at $T_c = 0.310$ K. R gives the measured values for THM02; the other devices are similar.

Material	L	W	t	V	Σ	$G_{\rm ep} = 5\Sigma V T^4$	R	$G_{\rm WF} = L_0 T/R$
	μm	μm	nm	$\rm m^3$	$\rm W/m^3K^4$	W/K	Ω	W/K
Bi (Abs.)	100	10	500	5.0×10^{-16}	0.24×10^9	5.5×10^{-9}		
Au (Abs.)	100	10	150	1.5×10^{-16}	$3.30 - 5.17 \times 10^9$	$2.3 - 3.6 \times 10^{-8}$		
Abs. total						$2.9 - 4.2 \times 10^{-8}$	2	0.38×10^{-8}
Au (TES)	20	10	190	0.38×10^{-16}	$3.30 - 5.17 \times 10^9$	$0.58 - 0.92 \times 10^{-8}$	0.35	2.2×10^{-8}

be suitable for low background measurements of millimeter waves for astrophysics.

ACKNOWLEDGMENTS

This work is supported by NASA CETDP award NAG5-10258.

REFERENCES

1. C. L. Bennett, R. S. Hill, G. Hinshaw, M. R. Nolta, N. Odegard, L. Page, D. N. Spergel, J. L. Weiland, E. L. Wright, M. Halpern, N. Jarosik, A. Kogut, M. Limon, S. S. Meyer, G. S. Tucker, and E. Wollack, "First-year wilkinson microwave anisotropy probe (wmap) observations: Preliminary maps and basic results," *Astrophysical Journal Suppl. Series* **148**, pp. 1–27, 2003.

Table 5. Expected values of the electronic heat capacity, C_e, and thermal time constant, τ_{ep}, for the devices we tested. Device dimensions appear in Table 4. Values are calculated at $T_c = 0.310$ K. The Sommerfeld constants, γ, are from Kittel.[17]

Material	γ J/K^2m^3	C_e J/K	$\tau_{ep} = C_e/G_{ep}$ s
Bi (Abs.)	0.398	0.62×10^{-16}	
Au (Abs.)	71	33.0×10^{-16}	
Abs. total		33.6×10^{-16}	$1.2 - 0.81 \times 10^{-7}$
Au (TES)	71	8.4×10^{-16}	$1.4 - 0.92 \times 10^{-7}$

2. J. M.Kovac, E. M.Leitch, C. Pryke, J. E. Carlstrom, N. W.Halverson, and W. L.Holzapfel, "Detection of polarization in the cosmic microwave background using dasi," *Nature* **420**, pp. 772–787, 2002.
3. A. Kogut, D. N. Spergel, C. Barnes, C. L. Bennett, M. Halpern, G. Hinshaw, N. Jarosik, M. Limon, S. S. Meyer, L. Page, G. S. Tucker, E. Wollack, and E. L. Wright, "First-Year Wilkinson Microwave Anisotropy Probe (WMAP) Observations: Temperature-Polarization Correlation," *Astrophysical Journal Suppl. Series* **148**, pp. 161–173, 2003.
4. K. D. Irwin, "An application of electrothermal feedback for high resolution cryogenic particle detection," *Appl. Phys. Lett.* **66**, pp. 1998–2000, 1995.
5. A. T. Lee, S. F. Lee, J. M. Gildemeister, and P. L. Richards, "Voltage-biased superconducting bolometers for infrared and mm-wave astronomy," in *Proc. LTD-7 Munich*, p. 123, 1997.
6. M. Gershenson, D. Gong, T. Sato, B. S. Karasik, and A. V. Sergeev, "Millisecond electronphonon relaxation in ultrathin disordered metal films at millikelvin temperatures," *Appl. Phys. Lett.* **79**, pp. 2049–2051, 2001.
7. A. F. Andreev *Sov. Phys. JETP.* **19**, p. 1228, 1964.
8. F. Pobell, *Matter and Methods at Low Temperature, 2nd Ed.*, Springer, Berlin-Heidelberg, 1996.
9. F. C. Wellstood, C. Urbina, and J. Clarke, "Hot-electron limitation to the sensitivity of the dc superconducting quantum interference device," *Appl. Phys. Lett.* **54**, pp. 2599–2601, 1989.
10. M. J. Myers, A. T. Lee, P. L. Richards, D. Schwan, J. T. Skidmore, A. D. Smith, H. Spieler, and J.Yoon, "Antenna-coupled arrays of voltage -biased superconducting bolometers," in *Low Temperature Detectors*, F. S.Porter, D.McCammon, M.Galeazzi, and C.K.Stahle, eds., *AIP Conf. Proc.* **605**, p. 247, 2002.
11. A. Goldin, J. J. Bock, C. Hunt, A. E. Lange, H. LeDuc, A. Vayonakis, and J. Zmuidzinas, "SAMBA: Superconductiong antenna coupled, Multifrequency,bolometric array," in *Low Temperature Detectors*, F. S.Porter, D.McCammon, M.Galeazzi, and C.K.Stahle, eds., *AIP Conf. Proc.* **605**, pp. 251–255, 2002.
12. D. Filipovic, G. Gauthier, S. Raman, and G. Rebeiz, "Off-axis properties of silicon and quartz dielectric lens antennas," *IEEE Trans. Antennas Propagat* **45**, pp. 760–766, May 1997.
13. C. A.Allen, D. J. Benford, J. A. Chervenak, W. Hsieh, R. A. McClanahan, R. M. T. M. Miller, S. H. Moseley, J. Staguhn, and T. R. Stevenson, "A dry-etch process for low temperature superconducting transition edge sensors for far infrared bolometer arrays," *Nucl. Instr. Meth in Phys. Res. A* **520**, 2004.
14. S. Ali, L. D. Cooley, D. McCammon, K. Nelms, J.Peck, D. Prober, D.Swetz, P. Timbie, and D. der Weide, "Planar antenna-coupled transition-edge hot electron microbolometer," *IEEE-Trans. Appl. Supercond.* **13**, p. 184, 2003.
15. F. Pierre, A. B. Gougam, A. Anthore, H. Pothier, D. Esteve, and N. Birge, "Dephasing of electrons in mesoscopic metal wires," *PRB* **68**, p. 085413, 2003.
16. S. I. Dorozhkin, F. Lell, and W. Schoepe, "Energy relaxation of hot electrons and inelastic collision time in thin metal films at low temperatures," *Solid State Communications* **60(3)**, pp. 245–248, 1986.
17. C. Kittel, *Introduction to Solid State Physics*, Wiley, John & Sons, Incorporated, 1995.